Artificial neural network model of hardness, porosity and cavitation erosion wear of APS deposited Al2O3 -13 wt% TiO2 coatings

Artificial neural network model of hardness, porosity and cavitation erosion wear of APS deposited Al_2O_3 -13 wt% TiO_2 coatings

M Szala[1], M Awtoniuk[2], L Łatka[3], W Macek[4] and R Branco[5]

[1] Lublin University of Technology, Faculty of Mechanical Engineering, Department of Materials Engineering, 36D Nadbystrzycka Street, Lublin 20-618, Poland
[2] Warsaw University of Life Sciences, Institute of Mechanical Engineering, 164 Nowoursynowska Street, 02-787 Warsaw, Poland
[3] Wrocław University of Science and Technology, Faculty of Mechanical Engineering, 5 Łukasiewicza Street, Wrocław 50 371, Poland
[4] University of Occupational Safety Management in Katowice, 8 Bankowa Street, 40-007 Katowice, Poland
[5] University of Coimbra, CEMMPRE, Department of Mechanical Engineering, Rua Luís Reis Santos, Pinhal de Marrocos, 3030-788 Coimbra, Portugal

m.szala@pollub.pl

Abstract. The aim of the article is to build-up a simplified model of the effect of atmospheric plasma spraying process parameters on the deposits' functional properties. The artificial neural networks were employed to elaborate on the model and the Matlab software was used. The model is crucial to study the relationship between process parameters, such as stand-off distance and torch velocity, and the properties of Al_2O_3-13 wt% TiO_2 ceramic coatings. During this study, the coatings morphology, as well as its properties such as Vickers microhardness, porosity, and cavitation erosion resistance were taken into consideration. The cavitation erosion tests were conducted according to the ASTM G32 standard. Moreover, the cavitation erosion wear mechanism was presented. The proposed neural model is essential for establishing the optimisation procedure for the selection of the spray process parameters to obtain the Al_2O_3-13 wt% TiO_2 ceramic coatings with specified functional properties.

1. Introduction

Among other methods, plasma spraying, or more precisely, atmospheric plasma spraying (APS) is the most commonly used technique of thermal spray in the industry. The APS gives many advantages, like good adhesion strength, high plasma jet temperature, and a relatively high deposition rate [1–3]. This allows the deposition of the ceramic materials, metallic coatings, or composite structures [4–6]. In the APS process, there are many parameters, which influence different power on the coatings' properties and its quality. However, there is a systematic need to optimise the spray parameters to obtain a required coatings' functional properties, likewise the resistance to various deterioration processes such as wear, corrosion, or erosion.

One of the less investigated damage-process is erosion taking place due to fluid unsteady flow or vibrations that indicated the cavitation field. Overall, cavitation erosion is a materials deterioration

process that has a mainly mechanical nature. Cavitation damage effectively speeds up by the presence of corrosion [7,8], solid particles [9–11], or both [9,12,13]. The literature of the subject presents the standardised test rigs used for cavitation erosion testing. These facilities operates according to the ASTM G32 (vibratory apparatus) [14,15], ASTM G134 (cavitating liquid jet) [16,17], or non-standard facilities [18–20]. However, laboratory testing is usually a time-consuming process. Therefore, to shorten the testing time or limits the samples' amount the various attempts were undertaken. Exemplary the materials cavitation erosion resistance (CER) evaluation can be explained on the investigation done in the incubation stage of erosion [21–24]. Overall, there is a need for correlating the mechanical and functional properties of the engineering materials with their CER. Thus, different attempts were taken, starting from the simple competitive analysis [25–27], application of regression methods [28–30], or usage of the artificial neural network (ANN) [31,32]. However, the ANN analysis should be preceded by specific phenomena modelling. Therefore, ANN modelling is still an up-to-date approach for many disciplines of engineering and science such as electrical engineering [33], mechanical engineering [34–36], pharmacology, and pharmacy [37,38], and many more. Although there are limited papers regarding the modelling and simulation of the CER of ceramic coatings. Even the literature presents competitive analysis into the effect of plasma spray parameters on the CER [39,40], according to the authors' knowledge, there is no work that utilises the ANN to predict the CER of APS thermally sprayed Al_2O_3-13 wt% TiO_2 ceramic coatings.

The aim of the paper is to build a neural model that connects APS process parameters with the properties of the Al_2O_3-13 wt% TiO_2 ceramic coatings. The model is crucial to investigate the relationship between process parameters and coatings properties. The overall idea of the paper continues the authors' goal, undertaken in the previous paper [32], aiming to describe the cavitation erosion process with the usage of ANN procedures.

2. Materials and Methods

2.1. Deposition and testing of the atmospheric plasma sprayed coatings

The atmospheric plasma spray process was employed to fabricate the Al_2O_3-13 wt% TiO_2 ceramic coatings. The details of the APS process description, as well as additional information, could be found, e.g. in [41,42]. The APS process was conducted with an SG100 plasma torch (Praxair, IN, USA), which was mounted on the 6-axis industrial robot Fanuc 2000 IA. The set of coatings was prepared with the usage of selected spraying process parameters namely, stand-off distance (h) and torch velocity (V), Table 1. In the APS process, the primary plasma gas was argon, while secondary gas was hydrogen. The deposition process was robotised in order to control all important parameters and to ensure repeatability.

The coatings surface and cross-sectional microstructure, hardness H (HV0.1), and porosity P, (%) were evaluated according to the procedures described in our previous papers [5,43,44] and obtained results were discussed in detail in the previously published paper [40]. The cavitation erosion resistance (CER) tests were conducted according to the ASTM G32 [45] standard using the vibratory test rig described elsewhere [25,40]. Overall, the CER test was conducted with usage of the stationary specimen method and the gap between the horn tip and sample surface that equals 1±0.05 mm. The cavitation worn samples were compared with the un-damaged surfaces using the scanning electron microscopy (SEM).

Table 1. Sample codes and variable APS process parameters.

Sample code	Stand-off distance, h (mm)	Torch velocity, V ($mm \cdot s^{-1}$)
AT13-1	80	300
AT13-2	80	500
AT13-3	90	400
AT13-4	100	300
AT13-5	100	500

2.2. The artificial neural network modelling procedure

The ANN model was prepared in the Neural Network Toolbox in Matlab (2017a). The block diagram of the model is shown in Figure 1. There were two input signals, i.e. stand-off distance, h (mm), torch velocity, V (mm·s^{-1}), and three output signals, i.e. hardness, H (HV0.1), porosity, P (%) and mean depth of erosion, MDE (μm). The overall idea of the model is a continuation of the authors' goal, undertaken in the previous paper [32] to analyse the erosion process with ANN methods.

The ANN model consists of three layers: input, hidden, and output. Each of the layers is attributed to a specific number of neurons. For example, the model denoted as 2-5-3 means a network with two input neurons, five hidden neurons, and three output neurons. The number of signals used in modelling determines the number of input and output neurons. The choice of the number of hidden neurons remains the decision-making parameter. We have chosen the size of the hidden layer experimentally by evaluating the performance of networks of different structures. Details of this analysis will be described in the Results and Discussion section. We have used the Levenberg-Marquardt backpropagation algorithm to train the network. The maximum number of epochs for training the network was equal to 40. Our dataset was limited to 5 samples only therefore, we decided to perform k-fold cross-validation. We assumed $k = n$, so it is a type of the so-called leave-one-out cross-validation [46].

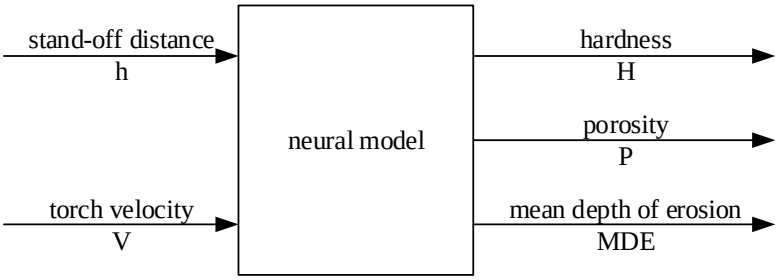

Figure 1. Model block diagram.

We used root mean square error NRMSE (informally called fit – this is the name we will use further) as a model performance evaluation index. The model describes the phenomenon in more detail if the fit value is higher. The fit index is calculated as follows:

$$fit = \left(1 - \frac{\|y - \hat{y}\|_2}{\|y - \bar{y}\|_2}\right) \cdot 100\% \quad (1)$$

where: y – output signal (measured), $\hat{y}$ – predicted output signal, $\bar{y}$ – mean of output (measured) signal.

3. Results and Discussion

3.1. Coatings properties and their cavitation erosion damage

This paper continuities the authors' recent attempt in the field of modelling of the structural materials and surface treatment for obtaining the required functional properties. In this research, the Al_2O_3-13 wt% TiO_2 ceramic coatings surface morphology and microstructure are presented in Figure 2, while the detailed hardness, porosity, and cavitation erosion resistance (CER) results are given in the authors' previous paper [40]. Briefly, the hardness of the ceramic coating was in the range of 885 HV0.1 up to 1235 HV0.1, porosity ranging from 5.59 % to 2.30 % and the CER results represented by MDE parameter for AT13-1; AT13-2; AT13-3; AT13-4 and AT13-5 equals 12.22 μm; 12.60 μm; 10.83 μm; 14.61 μm and 11.34 μm, respectively. The morphology of the cavitation-worn surfaces is presented in Figure 3. The current studies reviled that the fabricated APS coatings have the microstructure and as-sprayed surface morphology typical as for thermally sprayed coatings [47–49]. The lamellar splats, porosity, presence of not fully melted feedstock power particles of a semi-spherical shape, and cracking in the ceramic lamellas are visible in Figure 2. Each splat consists of columnar crystals which are

characteristic for APS deposited ceramics [40,50,51]. According to our previous study [40], the decreasing hardness derives from a less compact microstructure and a lower degree of fully molten particles. The quantitative cavitation results indicate the highest CER of AT13-3 samples, which obtained the lowest erosion rate and MDE [40]. Overall damage-mechanism relies on the removal of loosely material, surface non-uniformities, material discontinuities (e.g. partly melted particles), and spallation of splat-edges. Typically, the material discontinuities such as pores act as centres of material removal [25,39,43] and the wear process ends in coating material removal and the crater's creation towards the stainless steel substrate. For all deposited samples, the cavitation erosion behaviour relies on the brittle cracking that proceeds through the splat columnar-grains, see Figure 3.

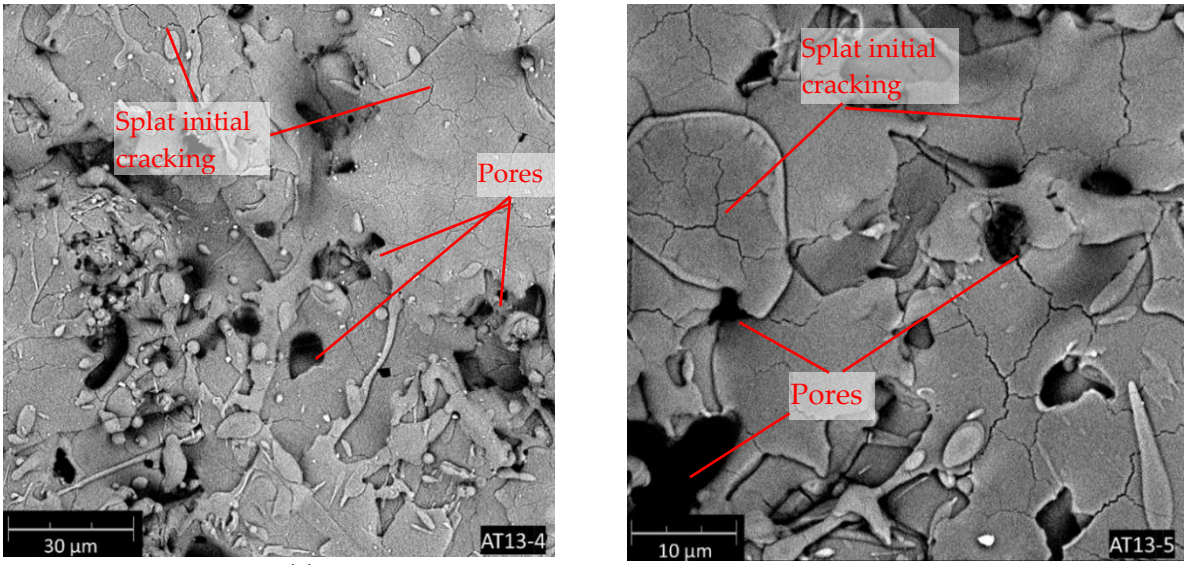

(a) (b)

Figure 2. APS as-deposited Al_2O_3-13%TiO_2 surface morphology of coatings: AT13-4 (a) and AT13-5 (b), SEM-BSD.

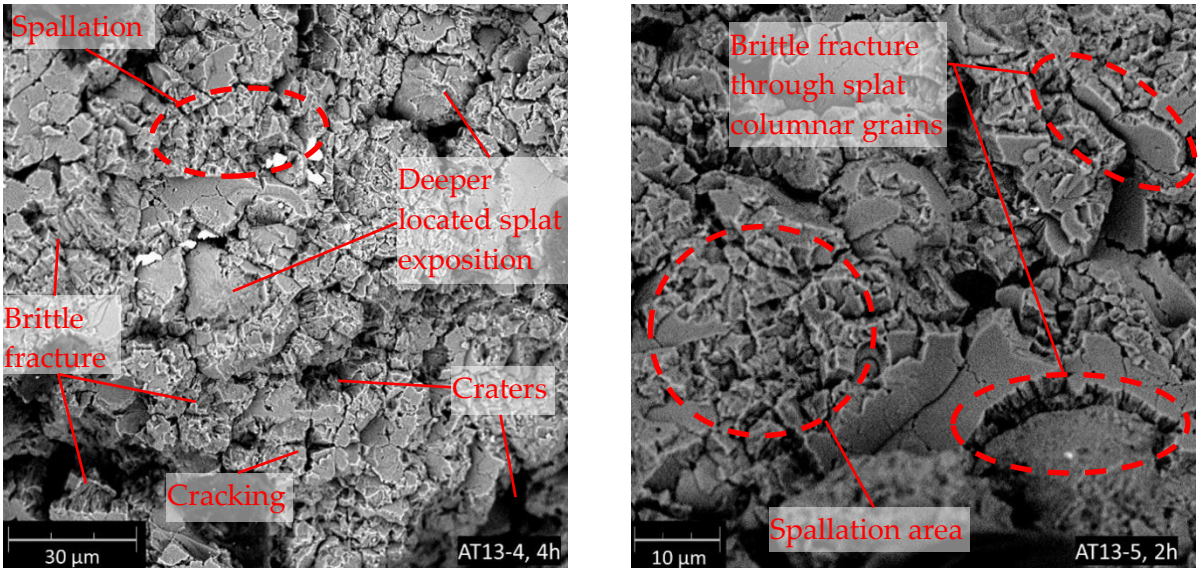

(a) (b)

Figure 3. Cavitation damage at different magnifications and exposure times: (a) erosion of AT13-4 after 4 h of cavitation, SEM; (b) erosion of coating AT13-5 after 2 h of cavitation testing, SEM-BSD.

3.2. *Modelling of hardness, porosity and cavitation erosion wear of the APS coatings*

The work base on the analysis of the data and method undertook in previously published papers [32,40]. In the current paper, the new ANN model was proposed. Figure 4 shows the relationship between the number of neurons in the hidden layer and model performance. For each output signal, the fit index was counted separately. Considering the learning dataset, it can be seen that a network with six or more neurons in the hidden layer perfectly (fit = 100%) matches the measurement data. In the case of the testing dataset, the situation is more complex. Usually, the network had the best fit to hardness H and the worst to mean depth of erosion MDE. Considering the results for both the learning and testing dataset, we have chosen a network with the structure 2-6-3, i.e. with six neurons in the hidden layer. The fit index values for the selected network are shown in Table 2.

Using the ANN model, we have performed a series of simulations of the APS thermal spray process. Stand-off distance h changed in the range 80-100 mm with a step of 1 mm and the velocity torch range changed in the range 300-500 mm·s^{-1} with a step of 10 mm·s^{-1}. Figure 5 shows the simulation results.

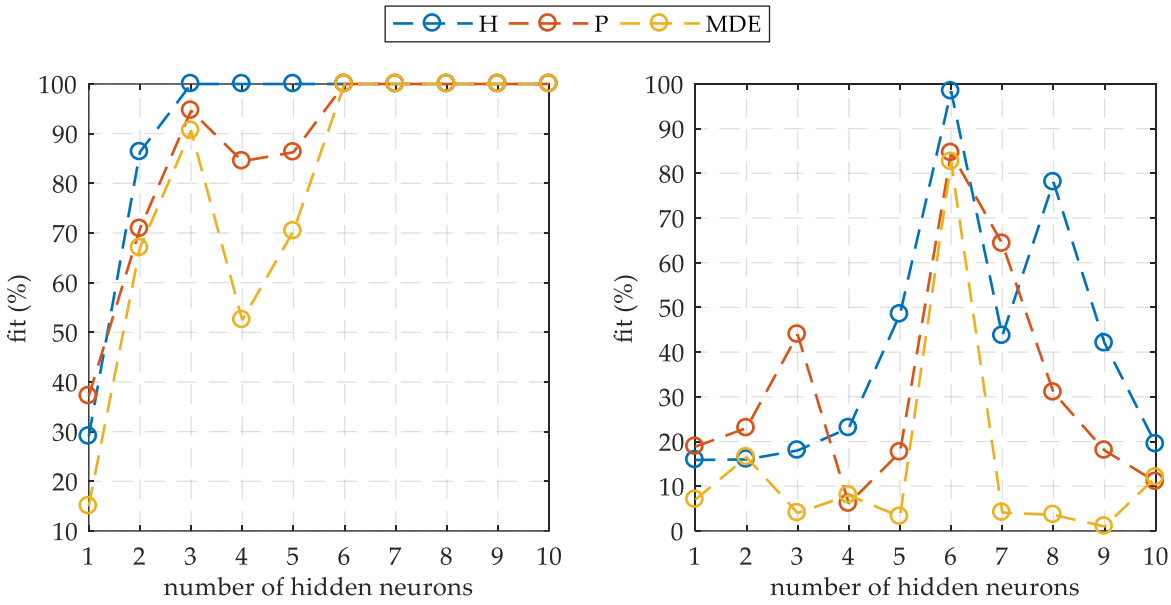

(a) (b)

Figure 4. Influence of the number of hidden neurons on the fit index for learning (a) and testing (b) dataset.

Table 2. The values of the fit index for ANN with 2-6-3 structure.

Output signal	Fit index (%)	
	Learning dataset	Testing dataset
H	100	98.4
P	100	84.6
MDE	100	82.6

In the APS process, the desired coatings are those with high hardness, low porosity, and high cavitation erosion resistance (red circles in Figure 5). Simulation studies have shown there is no common range of parameters h and V, which would guarantee a coating with all of the required properties.

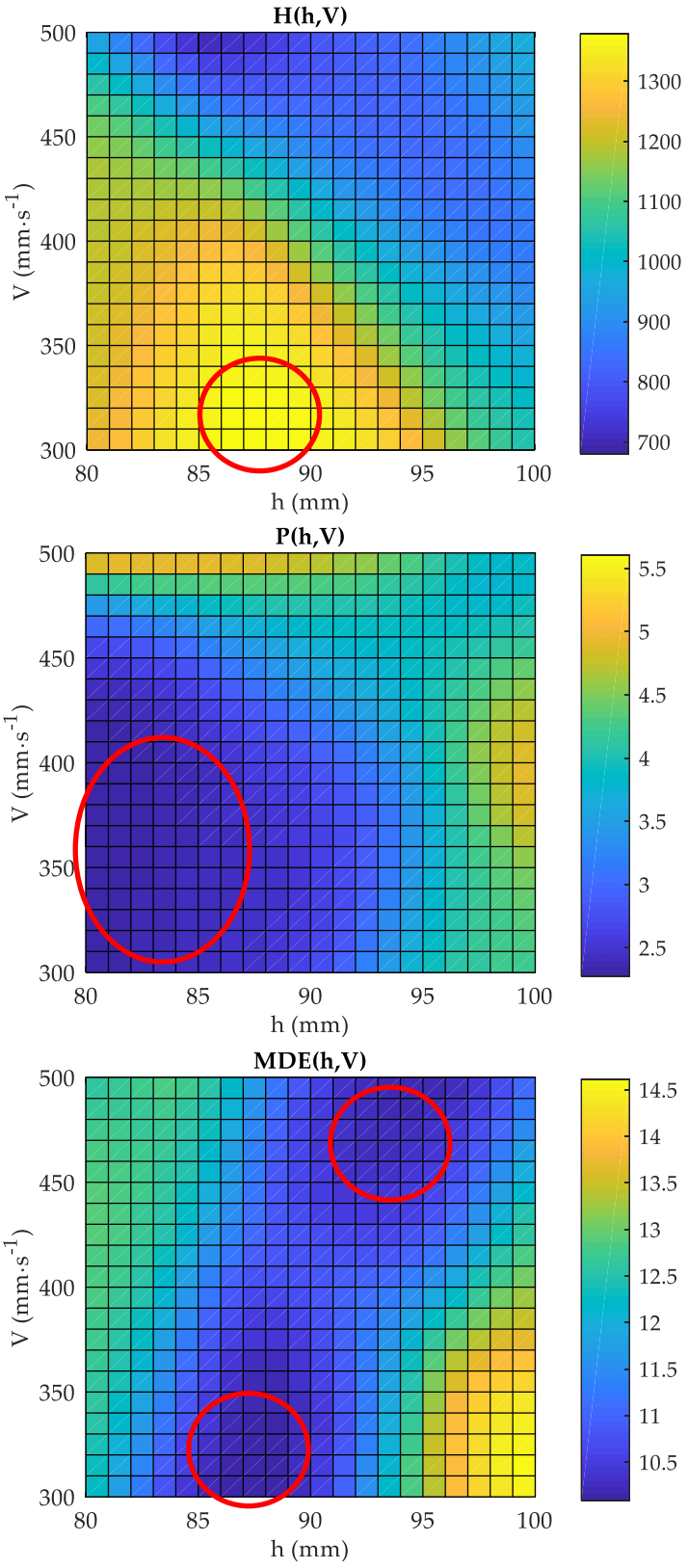

Figure 5. Contour plots of functions H(h,V), P(h,V) and MDE(h,V); the required properties of the coatings are marked in red.

The proposed ANN model is essential for establishing the procedure for the selection of the spray process parameters to obtain the Al_2O_3-13 wt% TiO_2 ceramic coatings with specified functional properties. This issue is further discussed in detail in the in-print-paper, see [52] that refers to neural modelling of APS thermal spray process parameters for optimising the hardness, porosity, and cavitation erosion resistance of AT13 coatings.

4. Conclusions

This paper presents the original ANN model that synthesises the atmospheric plasma spray (APS) process parameters and functional properties of Al_2O_3-13 wt% TiO_2 ceramic coatings. The results of the study lead to the following conclusions:

1. The ANN model is an appropriate tool to investigate the impact of APS process parameters (stand-off distance and torch velocity) on coatings properties (hardness, porosity, and cavitation erosion resistance).
2. A model can be implemented for the optimisation of the Al_2O_3-13 wt% TiO_2 coatings functional properties. To recognise the APS process parameters which ensure the optimum of coating properties, the model requires the application of a multi-criteria optimisation algorithm. This will be studied in our future research.
3. The APS ceramic coatings present relatively dense lamellar microstructure with initial cracks of lamellas, contain unmelted feedstock powder, and the splats which are build up from columnar grains. Coatings hardness ranges from 885 HV0.1 to 1235 HV0.1 and the porosity that equals from 5.59% to 2.30%. The AT13-3 sample deposited with process parameters: h = 90 mm and V = 400 $m \cdot s^{-1}$ presents the highest cavitation erosion resistance.
4. The cavitation erosion mechanism of the coatings relies on brittle mode. Fracture proceeds through the splat columnar grains besides is accelerated by the coatings nonuniformities, e.g. pores, cracks, not fully melted material.

Acknowledgements

The research was financed in the framework of the project Lublin University of Technology—Regional Excellence Initiative, funded by the Polish Ministry of Science and Higher Education (contract No. 030/RID/2018/19).

References

[1] Pawlowski L 2008 *The Science and Engineering of Thermal Spray Coatings* (Chichester, England ; Hoboken, NJ: Wiley)
[2] Łatka L, Szala M, Macek W and Branco R 2020 Mechanical Properties and Sliding Wear Resistance of Suspension Plasma Sprayed YSZ Coatings *Adv. Sci. Technol. Res. J.* **14** 307–14
[3] Fauchais P L, Heberlein J V R and Boulos M 2014 *Thermal Spray Fundamentals: From Powder to Part* (Springer US)
[4] Alontseva D L, Ghassemieh E, Voinarovych S, Russakova A, Kyslytsia O, Polovetskyi Y and Toxanbayeva A 2020 Characterisation of the microplasma spraying of biocompatible coating of titanium *J. Microsc.* **279** 148–57
[5] Maruszczyk A, Dudek A and Szala M 2017 Research into Morphology and Properties of TiO2 – NiAl Atmospheric Plasma Sprayed Coating *Adv. Sci. Technol. Res. J.* **11** 204–10
[6] Kiilakoski J, Musalek R, Lukac F, Koivuluoto H and Vuoristo P 2018 Evaluating the toughness of APS and HVOF-sprayed Al2O3-ZrO2-coatings by in-situ- and macroscopic bending *J. Eur. Ceram. Soc.* **38** 1908–18
[7] Chmiel J, Jasionowski R and Zasada D 2015 Cavitation erosion and corrosion of pearlitic gray cast iron in non-standardized cavitation conditions *Solid State Phenom.* **225** 19–24
[8] Cui Z D, Man H C, Cheng F T and Yue T M 2003 Cavitation erosion–corrosion characteristics of laser surface modified NiTi shape memory alloy *Surf. Coat. Technol.* **162** 147–53

[9] Amarendra H J, Chaudhari G P and Nath S K 2012 Synergy of cavitation and slurry erosion in the slurry pot tester *Wear* **290–291** 25–31
[10] Wang Y, Wu J and Ma F 2018 Cavitation–silt erosion in sand suspensions *J. Mech. Sci. Technol.* **32** 5697–702
[11] Su K, Wu J and Xia D 2020 Classification of regimes determining ultrasonic cavitation erosion in solid particle suspensions *Ultrason. Sonochem.* **68** 105214
[12] Silva F N da, Oliveira P M de, Araújo N M da F T de S, Carvalho Filho E T de, Cunha J D da, Silva D R da and Medeiros J T N de 2019 Corrosion-cavitation-erosion: surface morphology study of a carbon steel in a multiphasic saline bath *Matér. Rio Jan.* **24**
[13] Liang L, Pang Y, Tang Y, Zhang H, Liu H and Liu Y 2019 Combined wear of slurry erosion, cavitation erosion, and corrosion on the simulated ship surface *Adv. Mech. Eng.* **11** 1687814019834450
[14] Tocci M, Pola A, Girelli L, Lollio F, Montesano L and Gelfi M 2019 Wear and Cavitation Erosion Resistance of an AlMgSc Alloy Produced by DMLS *Metals* **9** 308
[15] Hattori S and Ishikura R 2010 Revision of cavitation erosion database and analysis of stainless steel data *Wear* **268** 109–16
[16] Steller J 1999 International Cavitation Erosion Test and quantitative assessment of material resistance to cavitation *Wear* **233–235** 51–64
[17] Szala M, Dudek A, Maruszczyk A, Walczak M, Chmiel J and Kowal M 2019 Effect of atmospheric plasma sprayed TiO2-10% NiAl cermet coating thickness on cavitation erosion, sliding and abrasive wear resistance *Acta Phys. Pol. A* **136** 335–41
[18] Jasionowski R, Przetakiewicz D and Przetakiewicz W 2014 Cavitation Erosion Resistance of Alloys Used in Cathodic Protection of Hulls of Ships *Arch. Metall. Mater.* **59** 241–245
[19] Mann B S and Arya V 2002 An experimental study to corelate water jet impingement erosion resistance and properties of metallic materials and coatings *Wear* **253** 650–61
[20] Krella A K and Zakrzewska D E 2018 Cavitation Erosion – Phenomenon and Test Rigs *Adv. Mater. Sci.* **18** 15–26
[21] García G L, López-Ríos V, Espinosa A, Abenojar J, Velasco F and Toro A 2014 Cavitation resistance of epoxy-based multilayer coatings: Surface damage and crack growth kinetics during the incubation stage *Wear* **316** 124–32
[22] Dular M, Bachert B, Stoffel B and Sirok B 2004 Relationship between cavitation structures and cavitation damage *Wear* **257** 1176–1184
[23] Szala M 2017 Application of computer image analysis software for determining incubation period of cavitation erosion – preliminary results *ITM Web Conf.* **15** 06003
[24] Gireń B G 2006 *Kawitacyjne niszczenie warstw ukształtowanych wiązką promieniowania laserowego* (Gdańsk: Wydawn. IMP PAN)
[25] Szala M, Łatka L, Walczak M and Winnicki M 2020 Comparative Study on the Cavitation Erosion and Sliding Wear of Cold-Sprayed Al/Al2O3 and Cu/Al2O3 Coatings, and Stainless Steel, Aluminium Alloy, Copper and Brass *Metals* **10** 856
[26] Will C R, Capra A R, Pukasiewicz A G M, Chandelier J da G and Paredes R S C 2012 Comparative study of three austenitic alloy with cobalt resistant to cavitation deposited by plasma welding *Weld. Int.* **26** 96–103
[27] Maksimović V M, Devečerski A B, Došen A, Bobić I, Erić M D and Volkov-Husović T 2017 Comparative Study on Cavitation Erosion Resistance of A356 Alloy and A356FA5 Composite *Trans. Indian Inst. Met.* **70** 97–105
[28] Lugscheider E, Barimani C, Eckert P and Eritt U 1996 Modeling of the APS plasma spray process *Comput. Mater. Sci.* **7** 109–14
[29] Hattori S, Ishikura R and Zhang Q 2004 Construction of database on cavitation erosion and analyses of carbon steel data *Wear* **257** 1022–9

[30] Tzanakis I, Bolzoni L, Eskin D G and Hadfield M 2017 Evaluation of Cavitation Erosion Behavior of Commercial Steel Grades Used in the Design of Fluid Machinery *Metall. Mater. Trans. A* **48** 2193–206
[31] Gao G, Zhang Z, Cai C, Zhang J and Nie B 2019 Cavitation Damage Prediction of Stainless Steels Using an Artificial Neural Network Approach *Metals* **9** 506
[32] Szala M and Awtoniuk M 2019 Neural modelling of cavitation erosion process of 34CrNiMo6 steel *IOP Conf. Ser. Mater. Sci. Eng.* **710** 012016
[33] Salat R and Awtoniuk M 2015 Black box modeling of PIDs implemented in PLCs without structural information: a support vector regression approach *Neural Comput. Appl.* **26** 723–734
[34] Winiczenko R, Sałat R and Awtoniuk M 2013 Estimation of tensile strength of ductile iron friction welded joints using hybrid intelligent methods *Trans. Nonferrous Met. Soc. China* **23** 385–391
[35] Kosowski K, Tucki K and Kosowski A 2010 Application of Artificial Neural Networks in Investigations of Steam Turbine Cascades *J. Turbomach.* **132**
[36] Kulisz M, Zagórski I, Matuszak J and Kłonica M 2020 Properties of the Surface Layer After Trochoidal Milling and Brushing: Experimental Study and Artificial Neural Network Simulation *Appl. Sci.* **10** 75
[37] Sałat R and Sałat K 2015 Modeling analgesic drug interactions using support vector regression: a new approach to isobolographic analysis. *J. Pharmacol. Toxicol. Methods* **71** 95–102
[38] Sałat R and Sałat K 2013 The application of support vector regression for prediction of the antiallodynic effect of drug combinations in the mouse model of streptozocin-induced diabetic neuropathy *Comput. Methods Programs Biomed.* **111** 330–337
[39] Jafarzadeh K, Valefi Z and Ghavidel B 2010 The effect of plasma spray parameters on the cavitation erosion of Al2O3–TiO2 coatings *Surf. Coat. Technol.* **205** 1850–5
[40] Łatka L, Szala M, Michalak M and Pałka T 2019 Impact of atmospheric plasma spray parameters on cavitation erosion resistance of Al2O3-13%TiO2 coatings *Acta Phys. Pol. A* **136** 342–7
[41] Michalak M, Łatka L, Sokołowski P, Niemiec A and Ambroziak A 2020 The Microstructure and Selected Mechanical Properties of Al2O3 + 13 wt % TiO2 Plasma Sprayed Coatings *Coatings* **10** 173
[42] Łatka L, Niemiec A, Michalak M and Sokołowski P 2019 Tribological Properties of Al2O3 + TiO2 Coatings Manufactured by Plasma Spraying *Bimon. Tribol.* **283** 19–24
[43] Szala M, Walczak M, Łatka L, Gancarczyk K and Özkan D 2020 Cavitation Erosion and Sliding Wear of MCrAlY and NiCrMo Coatings Deposited by HVOF Thermal Spraying *Adv. Mater. Sci.* **20** 26–38
[44] Łatka L, Michalak M and Jonda E 2019 Atmospheric Plasma Spraying of Al2O3 + 13% TiO2 Coatings Using External and Internal Injection System *Adv. Mater. Sci.* **19** 5–17
[45] Anon 2010 *ASTM G32-10: Standard Test Method for Cavitation Erosion Using Vibratory Apparatus* (PA, USA: ASTM International: West Conshohocken, Philadelphia)
[46] Tangirala A K 2015 *Principles of system identification : theory and practice* (Boca Raton: CRC Press)
[47] Łatka L, Pawłowski L, Winnicki M, Sokołowski P, Małachowska A and Kozerski S 2020 Review of Functionally Graded Thermal Sprayed Coatings *Appl. Sci.* **10** 5153
[48] Meghwal A, Anupam A, Murty B S, Berndt C C, Kottada R S and Ang A S M 2020 Thermal Spray High-Entropy Alloy Coatings: A Review *J. Therm. Spray Technol.* **29** 857–93
[49] Yılmaz R, Kurt A O, Demir A and Tatlı Z 2007 Effects of TiO2 on the mechanical properties of the Al2O3–TiO2 plasma sprayed coating *J. Eur. Ceram. Soc.* **27** 1319–23
[50] Matikainen V, Niemi K, Koivuluoto H and Vuoristo P 2014 Abrasion, Erosion and Cavitation Erosion Wear Properties of Thermally Sprayed Alumina Based Coatings *Coatings* **4** 18–36
[51] Davis J R 2004 *Handbook of Thermal Spray Technology* (ASM International)
[52] Szala M, Łatka L, Awtoniuk M, Winnicki M and Michalak M 2020 Neural modelling of APS thermal spray process parameters for optimising the hardness, porosity and cavitation erosion resistance of Al2O3 -13 wt% TiO2 coatings *Processes* **8** 1544